Earth and Planetary Science Letters 443 (2016) 185–194

Contents lists available at ScienceDirect

Earth and Planetary Science Letters

www.elsevier.com/locate/epsl

Tidal dissipation in creeping ice and the thermal evolution of Europa

Christine McCarthy [a,*], Reid F. Cooper [b]

[a] Lamont-Doherty Earth Observatory, Columbia University, Palisades, NY, USA
[b] Department of Earth, Environmental and Planetary Sciences, Brown University, Providence, RI, USA

ARTICLE INFO

Article history:
Received 7 August 2015
Received in revised form 22 February 2016
Accepted 4 March 2016
Available online 25 March 2016
Editor: C. Sotin

Keywords:
ice
attenuation
dislocations
icy satellites
microstructure
anelasticity

ABSTRACT

The thermal and mechanical evolution of Europa and comparable icy satellites—the physics behind creating and sustaining a subsurface water ocean—depends almost entirely on the mechanical dissipation of tidal energy in ice to produce heat, the mechanism(s) of which remain poorly understood. In deformation experiments, we combine steady–state creep and low-frequency, small-strain periodic loading, similar conditions in which tectonics and tidal flexing are occurring simultaneously. The data reveal that the relevant, power-law attenuation in ice (i) is non-linear, depending on strain amplitude, (ii) is independent of grain size, and (iii) exceeds in absorption the prediction of the Maxwell solid model by an order of magnitude. The Maxwell solid model is widely used to model the dynamics of planetary ice shells, so this discrepancy is important. The prevalent understanding of damping in the geophysical context is that it is controlled by chemical diffusion on grain boundaries, which renders attenuation strongly dependent on grain size. In sharp contrast, our results indicate instead the importance of intracrystalline dislocations and their spatial interactions as the critical structural variable affecting dissipation. These dislocation structures are controlled by stress and realized by accumulated plastic strain. Thus, tectonics and attenuation are coupled, which, beyond the icy satellite/subsurface ocean problem, has implications also for understanding the attenuation of seismic waves in deforming regions of the Earth's upper mantle.

1. Introduction

Although water ice is one of the most common substances in the solar system, it is also one of the most enigmatic, with much remaining unknown about its viscoelastic properties. To interpret surface features of icy satellites and to model thermal evolution via tidal dissipation, a thorough understanding of the rheological properties of ice and ice-rich mixtures at planetary conditions is needed. Without such experimental data, processes on icy satellites typically have been modeled using a simple Maxwell solid or a steady–state rheology (e.g., Ojakangas and Stevenson, 1989). However, the disparity between predicted behavior using Maxwell's model and observed behavior from recent satellite-based measurements (e.g., geysers and tectonics) demonstrates the need to refine such models to include the spectrum of mechanical response from elastic to anelastic to viscous (Shoji et al., 2013). To account for significant heat generated by mechanical dissipation of tidal forces, a transient, anelastic response is required. Since microstructure influences transient/anelastic properties and steady–state behavior establishes and sustains microstructure, the overlap of transient and steady–state behavior is important for tidal processes. Further, the ability to extrapolate laboratory data to planetary dynamics requires understanding of the physics of dissipation and how it scales with frequency, grain size, and temperature, as well as with stress and accumulated strain.

On Europa, the global stress field within the icy shell includes a diurnal component with a frequency $f = 3 \times 10^{-6}$ Hz from periodic tidal flexing with a strain amplitude of $\sim 10^{-5}$ (Tobie et al., 2003). Additionally the presence of the liquid ocean decouples the shell, resulting in a significantly larger component of tidal stress from reorientation of the tidal bulge relative to the parent body's direction, called nonsynchronous rotation, which has a larger strain amplitude and much larger period ($\sim 10^{13}$ s) (Greenberg et al., 1998). In addition to these two periodic stresses, it is posited that convective overturn can occur within an icy shell creating a stress on the order of tens to hundreds of kPa (Pappalardo et al., 1998).

Here we describe and interpret the results from a series of experiments that measure the anelastic response of polycrystalline ice simultaneously experiencing a cyclic load and a constant steady–state load at realistic stress/strain amplitudes and at frequencies approaching those of satellite tides. The tests highlight the fact that different mechanisms act at different timescales: the

* Corresponding author.
E-mail address: mccarthy@ldeo.columbia.edu (C. McCarthy).

http://dx.doi.org/10.1016/j.epsl.2016.03.006
0012-821X/

mechanism rate-limiting high-strain creep need not be the same as that providing the relaxation of a small periodic perturbation. The beauty of attenuation is that it can be used as *mechanical spectroscopy* to see the mechanisms (via small disturbances) shrouded by the steady–state behavior.

2. Experimental method

In this study deformation experiments were conducted on polycrystalline ice samples. We used three different methods of sample preparation in order to obtain specimens with four distinct grain sizes: (1) coarse (C: $d \sim 300$ μm); (2) medium (M: $d \sim 150$ μm); (3) fine (F: $d \sim 20$ μm); and (4) very fine (VF: $d \sim 8$ μm). Those methods were: bulk solidification from seeded water to create C samples (McCarthy et al., 2007); nebulization of water with flash freezing followed by sieving to desired particle size and "hot"-pressing to create M and F samples (Goldsby and Kohlstedt, 1997); and ice-II to ice-I phase transformation via a pressure release protocol to create VF samples (Durham et al., 2001). The details of each fabrication method can be found in Appendix A.1. Sample characterization was conducted using a scanning electron microscope (SEM) fitted with a cryogenic preparation station. Secondary electron images (SEI) were taken of fresh fracture surfaces while remaining under vacuum with $T < 100$ K and a low accelerating voltage of 2 kV (Fig. 1). Sublimation rates in the SEM are known to be higher at grain boundaries, ostensibly etching the samples (Cullen and Baker, 2001). Grain size was measured for each of the VF, F, and C samples using the line intercept method on SEM images, with a correction factor of 1.5 (Gifkins, 1970). A total of 7 transects and 53 grains were counted from three VF sample images; 24 transects and 252 grains were counted from seven F sample images; and 5 transects and 28 grains were counted from one C sample image. The grain size errors listed parenthetically in Table 1 represent the standard deviation from the mean of these counts. Several samples were examined prior to deformation and after deformation and no discernable grain growth occurred during mechanical testing.

Using a commercial servomechanical-actuator testing apparatus that was modified for cryogenic conditions, samples were subjected to a sinusoidally time-varying compressive stress superposed upon a constant, median applied compressive stress. The resulting strain—a steady–state creep strain plus a periodic anelastic strain—was measured with a gravity-fed extensometer that, by specifications, could resolve differential strains of $\varepsilon = 5 \times 10^{-7}$; thermal noise limited the strain resolution to 5×10^{-6}. Complex modulus and attenuation Q^{-1} are measured from the amplitude ratio and the tangent of phase delay δ, respectively, of the peak stress σ and peak strain ε. (A detailed description of the apparatus and data analyses are provided in Appendix A.) In this study the tests employed uniaxial loading so that the properties measured were Young's modulus E and attenuation Q_E^{-1}. In most cases, the median applied stress was $\sigma_m = 1$ MPa (Table 1). For this median stress, and the temperatures and grain sizes of the majority of these samples, the steady–state flow was accomplished by grain boundary sliding that is strain-accommodated by basal dislocation slip (Goldsby and Kohlstedt, 2001), the mechanism thought to be most applicable to tectonic processes in the geophysical ice-shell problem (Barr and Showman, 2009). In the case of the coarsest-grain-sized specimens in this study, deformation conditions were instead consistent with dislocation creep. The range of applied stress sinusoids studied was $\sigma_0 = 0.05$–0.28 MPa (cyclic strain amplitude $\varepsilon_0 \approx 5 \times 10^{-6}$–$3 \times 10^{-5}$), with 0.167 ± 0.006 MPa (1.7×10^{-5}) being the amplitude used for most tests (and 0.16 MPa the value used for analyses). Testing was conducted in the temperature range $200 \le T(\mathrm{K}) \le 260$ and over the frequency range 10^{-4}–10^{-1} Hz. Error was determined by performing multiple tests

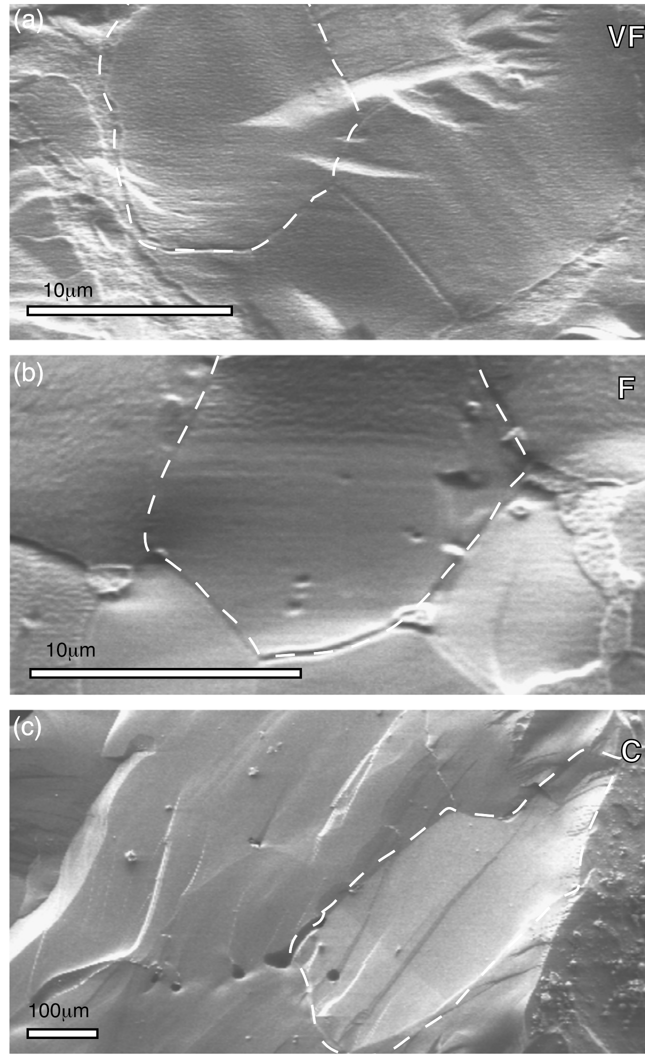

Fig. 1. SEM/SEI images of water ice-I made via three different fabrication techniques: (a) very fine-grained VF (8.4 ± 1.8 μm) made by pressure release method which results in subdivision of originally larger, spherical grains; (b) fine-grained F (19.9 ± 3.0 μm) prepared by droplet solidification, in which triple junctions and pronounced grain boundary troughs can be seen; and (c) coarse-grained C (300 ± 60 μm) grown slowly by bulk solidification in test tubes. A fourth grain size, medium-grained M (<180 μm) was also fabricated using the droplet solidification method (but a larger sieve), but was not imaged. Grain size for specimens M is estimated from the sieve size. A dashed white line in each figure roughly outlines a single grain.

(between three and five, depending on frequency) and plotting the mean value and absolute variation thereof.

3. Experimental results

The steady–state effective viscosities demonstrated by our specimens are consistent with those from previous experimental studies on similar polycrystalline specimens of ice-I (e.g., Goldsby and Kohlstedt, 2001). A typical creep curve from initial loading (prior to the periodic loading) is provided in the Appendix (Fig. A.2(a)). Fig. 2 presents the results of linearity tests, which were confined to the F (∼20 μm) specimens and run at $f = 0.01$ Hz. The median differential stress for all tests was $\sigma_m = 1$ MPa. The material demonstrates a modest strain-amplitude dependence of attenuation, $Q_E^{-1} \propto \varepsilon_0^{0.39}$, with the response insensitive to temperature, to first order.

Attenuation and Young's modulus data for the fine-grained (F) samples as a function of testing temperature are presented in Fig. 3. The data display clear temperature dependence, with, at